Evaluation of MRI Issues for a New Wirelessly Powered, Spinal Cord Stimulation Lead With Receiver

Laura P. Vasquez[1]
Ji Chen[2]
Frank G. Shellock[3]

OBJECTIVE. MRI is an imaging modality frequently ordered for patients with neuromodulation systems implanted for spinal cord stimulation. The purpose of this investigation was to evaluate MRI safety issues (magnetic field interactions, MRI-related heating, functional disturbances, and artifacts) for a new wirelessly powered lead with receiver used for SCS.

MATERIALS AND METHODS. Lead samples underwent in vitro evaluation for MRI safety issues using standardized techniques. Magnetic field interactions (i.e., translational attraction and torque) and artifacts were tested at 3 T. MRI-related heating was performed at 1.5 T/64 MHz and 3 T/128 MHz using two different methods: numerical simulations with analytical modeling and physical testing. Possible functional disturbances were evaluated under exposures to 1.5-T/64-MHz and 3-T/128-MHz MRI conditions.

RESULTS. The lead exhibited minor magnetic field interactions (22° deflection angle, no torque) at 3 T. The highest temperature change recorded at 1.5 T/64 MHz and 3 T/128 MHz was 3.8°C and 11.3°C, respectively. Exposures to MRI conditions did not damage or alter the functional aspects of the leads. The maximum artifact size seen on a gradient-echo pulse sequence extended approximately 10 mm relative to the size of the lead.

CONCLUSION. The MRI tests performed on patients with the new lead with receiver revealed no substantial concerns with respect to the conditions that we provide in the safety guidelines that were based on the results of this investigation. Therefore, MRI examinations will result in acceptable heating when conducted at appropriate whole-body-averaged specific absorption rate levels (i.e., 2.0 W/kg at 1.5 T/64 MHz and 0.3 W/kg at 3 T/128 MHz, corresponding to adjusted temperature rises of 3.6°C and 1.2°C, respectively). Therefore, patients with this wirelessly powered lead and receiver implanted can safely undergo MRI examinations under specific conditions.

Keywords: implants, MRI, MRI safety, neuromodulation, spinal cord stimulator (SCS)

doi.org/10.2214/AJR.19.21503

Received March 26, 2019; accepted after revision August 6, 2019.

[1]Department of Medical Imaging Sciences, Rush University, College of Health Sciences, 600 S Paulina St, Ste 764AAC, Chicago, IL 60612. Address correspondence to L. P. Vasquez (laura_vasquez@rush.edu).

[2]Department of Electrical and Computer Engineering, University of Houston, Houston, TX.

[3]Department of Radiology and Medicine, Keck School of Medicine, University of Southern California, Los Angeles, CA.

AJR 2020; 214:406–412

0361–803X/20/2142–406

More than 30% of Americans suffer from acute or chronic pain, affecting approximately 100 million adults in the United States, which is more than the total afflicted by heart disease, cancer, and diabetes combined [1, 2]. Chronic pain is the leading cause of physical ailments, emotional suffering, and disability. Causes include chronic back and leg pain, failed back surgery syndrome, complex regional pain syndrome, neck injuries, lumbar radiculopathy, degenerative spinal disease, and arthritis [3, 4]. The standard treatment for chronic pain not related to cancer includes surgical intervention, pharmacology (usually opioids), physical therapy, or some combination of those approaches [3–5].

Neuromodulation or spinal cord stimulation (SCS) has been used to treat intractable pain for more than 40 years, and its application is expected to rise for treatment of failed back surgery syndrome [1, 3, 4]. SCS therapy is considered to be a viable, cost-effective treatment of chronic pain because it reduces medical treatments, clinical visits, and opioid use [5–10].

Because of the nature of the neurologic conditions associated with use of SCS systems, the need to undergo MRI is likely to increase, and other conditions may also warrant assessment with this diagnostic modality [11, 12]. For example, Desai et al. [12] conducted an analysis on MRI utilization in patients with SCS implants and reported that up to 84% of patients will require at least one MRI procedure within 5 years of receiving the implant and as many as 74% of patients would require a non–spine-related MRI examination within 10 years. Furthermore, they reported that an estimated 87% of

patients with chronic back and leg pain will have other comorbid conditions that are optimally evaluated by MRI. These findings highlight the need for MR-conditional SCS systems that permit MRI examinations to be performed safely [12].

Traditional neuromodulation systems used for SCS consist of surgical implantation of the following basic components: an internal pulse generator, lead extensions, and an implanted lead with stimulating electrodes. Because of possible complications and hardware-related issues, the internal pulse generator (i.e., battery, circuitry, and antenna) used with these devices may pose a high risk for adverse events [7]. Because of the potential hazards that affect implants in association with MRI (e.g., movement or dislodgment of ferromagnetic objects, excessive heating of conducting materials, induction of currents, and functional damage), all active implantable medical devices, especially neuromodulation systems, require extensive testing to identify and characterize issues that may create risks to patients or damage the instrumentation [1, 13–19]. Notably, certain neuromodulation systems have been specially designed in consideration of the electromagnetic environment associated with MRI technology and are labeled MR conditional, allowing patients to undergo MRI if specific requirements that ensure their safety are followed. The standard of care for managing a patient referred for an MRI procedure with an implant or device is to consult the MRI-specific labeling of the implant or device. As the designs of these implants and devices improves, refined heat-related MRI simulations will be required for precise MR-conditional labeling [1, 15].

A new wirelessly powered lead with receiver used for SCS recently received approval from the U.S. Food and Drug Administration for the treatment of chronic pain. This SCS system is intended as either a sole mitigating device or as an adjunct to pain management therapy [9, 10, 17]. In comparison with traditional neuromodulation systems used for SCS, which often carry extensive restrictions for MRI examinations [1], this new system may have fewer limitations because of its design [9, 10]. Therefore, the purpose of this investigation was to use in vitro test methods to characterize magnetic field interactions, MRI-related heating, possible functional disturbances, and artifacts for this wirelessly powered lead with receiver.

Materials and Methods

Wirelessly Powered Lead With Receiver

This investigation evaluated MRI-related issues for a wirelessly powered lead with receiver (Freedom-8A Stimulator and Freedom Receiver, Stimwave Technologies) used for SCS. The device is composed of an implantable lead that is placed in the epidural space via a minimally invasive procedure and a portable external component that wirelessly transmits power to a miniaturized receiver embedded within the lead. The external component cannot be worn during an MRI examination, so it was not assessed for MRI-related issues.

The dimensions and features of the lead with receiver are as follows: length, 45 cm (metallic portion, 16 cm; plastic portion, 29 cm); diameter, 1.35 mm; and eight cylindric electrodes. The plastic portion of the lead can be trimmed as needed (the clinician will typically implant 25–30 cm of the total lead length) [9, 10]. The stimulator's electrodes are embedded in the plastic material (length, 3 mm spaced every 4 mm (Fig. 1). The materials used to make the lead with receiver include platinum-iridium, polyurethane, polyimide, copper, nickel-cobalt alloy, and lead-free solder.

Magnetic Field Interactions

The lead with receiver was evaluated for magnetic field interactions (i.e., translational attraction and torque) using a 3-T system (Excite, HDx, Software 14 ×.M5, GE Healthcare). The static magnetic field strength of 3 T was used because it represents the highest available level in widespread clinical use [15] (7 T is now approved in the United States for clinical MRI, but few of these higher- field-strength scanners are presently in use). Because a 1.5-T scanner has a lower static magnetic field strength than a 3-T scanner, the ferromagnetic qualities are less at that lower field strength.

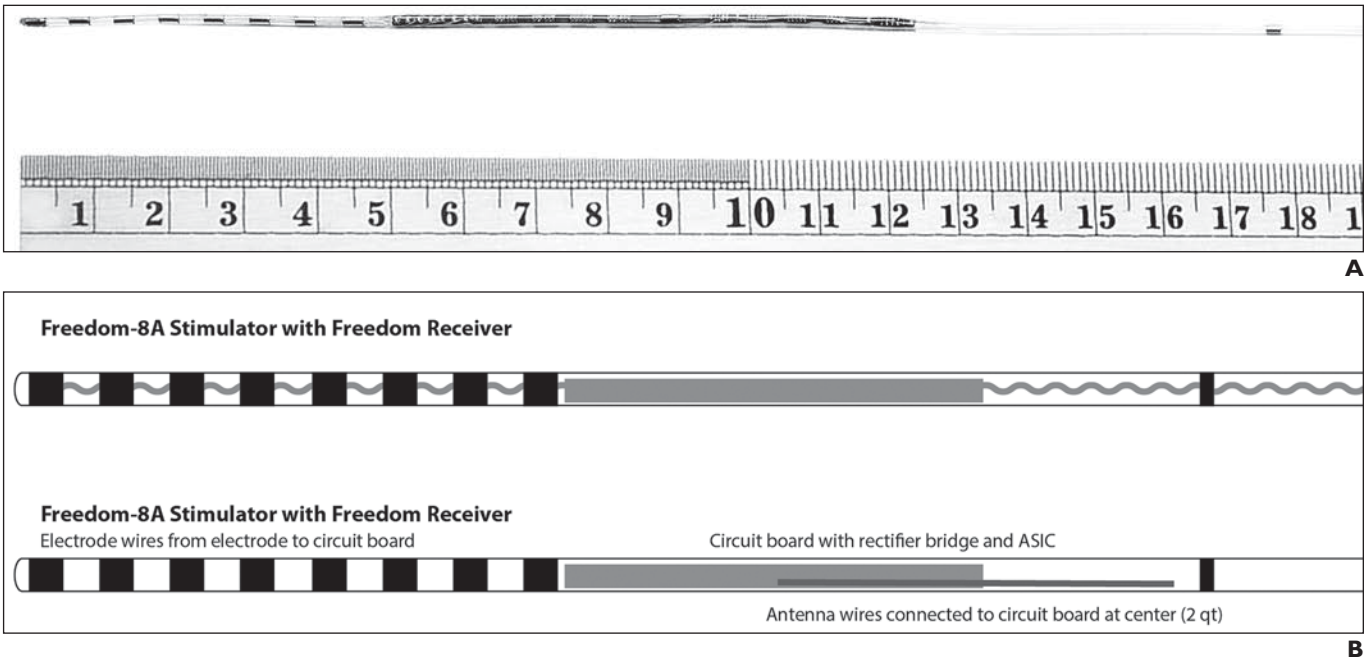

Fig. 1—Wirelessly powered lead with receiver used for spinal cord stimulation that underwent testing for MRI issues. (Courtesy of Stimwave Technologies, Inc.)
A, Photograph shows lead with receiver. Note incorporation of dipole antenna and contacts (i.e., electrodes). Scale is in centimeters.
B, Schematic shows details of lead with receiver. ASIC = application-specific integrated circuit, qt = quantity.

Translational attraction—The de ection angle test was used to determine translational attraction at 3 T for the lead with receiver as previously described [14, 17]. The test location for the de ection angle was at the opening of the bore of the MRI system, 74 cm from isocenter, on the central axis of the bore along the *z*-direction of the static magnetic eld [14]. This position was determined using a gauss meter (Extech Model 480823, Extech), which indicated a spatial gradient magnetic eld value of 466 G/cm, which is the highest value deemed "patient accessible" for the scanner. The de ection angle measured from the vertical direction to the nearest degree was measured three times, and a mean value was calculated.

Qualitative assessment of torque—A test apparatus made of at plastic material (i.e., with a low coef cient of friction) with a millimeter grid was used to qualitatively determine the presence of magnetic eld–induced torque for the lead with receiver, as previously described [17]. The test apparatus with the lead with receiver was positioned in the center of the MRI system, where the effect of torque is known to be the greatest [15, 17]. The lead with receiver was then moved 45° relative to its previous position and carefully observed for alignment or rotation relative to the direction of the static magnetic eld. This process was repeated to encompass a full 360° rotation for the device. The entire procedure was conducted three times, and a mean value was calculated [17]. The following qualitative scale was applied to the results [17]: 0, no torque; +1, mild or low torque, device slightly changed orientation but did not align to the magnetic eld; +2, moderate torque, device aligned gradually to the magnetic eld; +3, strong torque, device showed rapid and forceful alignment to the magnetic eld; +4, very strong torque, device showed both very rapid and forceful alignment to the magneti eld.

Assessment of MRI-Related Heating

The MRI-related heating evaluation incorporated recommendations and guidelines from the American Society for Testing and Materials (ASTM) International, the U.S. Food and Drug Administration, and standardized procedures obtained from the latest peer-reviewed literature [15, 17–22]. The comprehensive procedures were conducted under 1.5 T/64 MHz and 3 T/128 MHz because these are commonly used conditions in the clinical setting [15]. The MRI-related heating assessment consisted of a two-phase process: phase 1 consisted of numeric simulations and analytic modeling; phase 2, experimental testing.

Phase 1—Numerical simulations and analytic modeling were used to determine the highest (worst-case) temperature rises for the lead with receiver, taking into consideration its intended use during implantation in a human subject [19–21]. In this analysis, the spot that induced the highest temperature rise along the surface of the device was considered the position of maximum heating for this device and, thus, the most likely position of tissue damage if an excessive temperature rise occurred during MRI. The methods used were in accordance with described standardized procedures [20, 21].

Human body simulations were performed using human models from Virtual Population 3.0 (IT'IS Foundation) for biomedical applications. Virtual Population 3.0 is a set of computational models of independent anatomies including male and female sexes, with ages spanning from fetus to 84 years old and adult body mass indexes ranging from 21.7 to 36.2. To calculate the temperature distribution inside the body tissues, a human model characterized by body size, age, and sex can be simulated. In reality, a living human body generates blood ow, which removes some of the energy from the body and therefore may change temperature distribution. Such a bioheat effect can be considered by completing the thermal simulation for the human model with a bioheat transfer mechanism and including metabolism rate and blood ow formulations. This process provides a more realistic in vivo estimation. The simulation of the human model is performed with the goal of comparing the temperature measurement of the methodologic setup with the temperature increase in the human tissues, which is recommended in International Organization for Standardization Technical Standard ISO/TS 10974:2012 (for active implantable medical devices) and ASTM F2182–11a (for nonactive medical devices) [19–21].

For the rst part of phase 1 analysis, an ASTM International phantom was positioned within 64-MHz (for 1.5 T) and 128-MHz (for 3 T) transmit radiofrequency (RF) body coils. The center of the ASTM International phantom was placed at the isocenter of the transmit RF coil. For this simulation setup, the phantom was lled with gelled saline in accordance with ASTM International guidelines [18]. The gelling agent consisted of an aqueous solution of 1.32 g/L NaCl and 10 g/L polyacrylic acid (PAA) formula in distilled water. Using this formulation, the room-temperature (22°C) electrical conductivity of the gelled saline was 0.47 S/m, and the viscosity was suf cient to prevent convective heat transport [18].

SEMCAD X software (version 14.8, Aletsch) was used to obtain the electric eld distribution within the entire ASTM International phantom [19, 20]. The phantom was placed within a typical high-pass transmit RF coil with its electric eld distribution at the center transverse section plane of the coil. Electric eld distributions for most MRI whole-body transmit birdcage RF coils have similar patterns [18]. Testing methods were based on guidelines from ISO/TS 10974:2012 [19]. First, in vivo RF-induced energy was emitted to the lead with receiver inside the human model. Next, the incident electric eld along various trajectories (i.e., pathways) of the lead with receiver were computed according to well-accepted methods [19, 20]. These two computations included the trajectory exiting the thoracic spine at T8 and the trajectory exiting the lumbar spine at L1. Determination of the pathways for the lead with receiver were based on recommendations from physicians who had experience implanting the lead with receiver (Perryman L, oral communication, 2018).

The transfer function measurement was obtained by placing the ASTM International phantom within 64-MHz (for 1.5 T) and 128-MHz (for 3 T) whole-body RF coils. The lead with receiver was placed in the phantom along the rst trajectory at T8 and the second trajectory at L1. The electrical elds along these two trajectories were extracted after the completion of the human model simulations. Once these incident electric elds were projected, the tangential electric eld could be calculated and applied to predict the in vivo RF-induced voltage at the position of the distal electrode, also called the tip, of the lead with receiver [19–21].

The results were normalized to a whole body–averaged speci c absorption rate (SAR) of 2.0 W/kg with respect to the use of a transmit RF body coil used for MRI. This SAR value corresponds to the normal operating mode of operation for MRI systems [1, 15, 19]. Thus, these ndings provided rationale and guidance for the worst-case experimental testing setup that was used in phase 2.

Phase 2—MRI-related heating was evaluated for the lead with receiver at 1.5 T/64 MHz and 3 T/128 MHz. This procedure involved the use of a plastic ASTM International phantom that was lled to a depth of 10 cm with a semisolid gelled saline (i.e., 1.32 g/L NaCl plus 10 g/L polyacrylic acid in distilled water) [17, 18, 22, 23]. The lead with receiver was placed in a position in the phantom according to the results of the numeric simulations and analytic modeling to ensure a worst-case heating scenario, thus ensuring extreme RF heating conditions for this experimental setup [20, 21]. A relatively high level of RF energy was applied under each MRI condition during the MRI-related heating evaluations, as previously described [7, 22, 23]. Because this experimental setup lacks blood ow or tissue perfusion, it simulates an extreme condition used to assess heating for this lead with receiver.

MRI conditions—MRI was performed at 1.5 T/64 MHz (Magnetom, Siemens Healthcare) and

3 T/128 MHz (Excite, GE Healthcare). The transmit RF body coils were used to transmit RF energy. The landmark position for MRI was located at the center of the lead with receiver, with section locations obtained throughout the device. MRI parameters were selected to generate relatively high levels of RF energy, which was applied for 15 minutes [17, 18, 22, 23]. A system-reported, whole body–averaged SAR of 2.9 W/kg was applied at 1.5 T/64 MHz and a whole body–averaged SAR of 2.9 W/kg was applied at 3 T/128 MHz [17, 18, 22, 23].

Temperature recordings—Temperature recordings were obtained using a uoroptic thermometry system (Luxtron Model 3100 Fluoroptic Thermometry System, Lumasense) [22, 23]. The thermometry system has small (0.5-mm diameter) ber-optic probes (Model SFF-2) with an accuracy and resolution of 0.1°C. To properly record a representative highest temperature rise during each heating assessment, the uoroptic thermometry probe was placed on the lead with receiver on the basis of the analysis provided by the numerical simulations and analytic modeling. Thus, the thermometry probe was placed on the distal electrode of the lead with receiver. To record a reference temperature during the heating assessment, an additional thermometry probe was placed in the ASTM International phantom at a position removed from the lead (> 30 cm away from the lead on the opposite edge of the phantom [17, 22, 23]. This same positioning scheme was used for both heating evaluations.

MRI-related heating protocol—The gelled saline– lled phantom was placed in the 1.5-T/64-MHz and 3-T/128-MHz MRI systems rooms and equilibrated to the respective environmental conditions for more than 24 hours. Baseline (before MRI) temperatures were recorded at 4-second intervals for 5 minutes. MRI was then performed for 15 minutes, with temperatures recorded at 4-second intervals. After MRI was completed, temperatures were recorded at 4-second intervals for 2 minutes. The highest temperature changes recorded by the uoroptic thermometry probes are reported at 1.5 T/64 MHz and 3 T/128 MHz.

In additional, background temperatures (i.e., heating of the ASTM International phantom without the lead with receiver present) were recorded as part of the MRI-related heating assessments [17, 18, 22, 23]. Thus, the temperature changes were measured at the same positions used for the uoroptic thermometry probes and at the same time intervals used to record the temperatures for the lead with receiver.

The highest background temperature changes recorded during the evaluations at 1.5 T/64 MHz and 3 T/128 MHz also are reported. This testing method has been described in the literature and has been used for many assessments of implant heating related to MRI [15, 17, 22, 23].

Assessment of Possible Functional Disturbances

To determine if the lead with receiver exhibited a change in function or sustained damage associated with different MRI conditions, evaluations of the effects of exposures to different MRI conditions at 1.5 T/64 MHz and 3 T/128 MHz were performed, as previously described [23]. Thus, various MRI exposures and conditions were applied to the samples of the lead with receiver to reproduce common clinical scenarios associated with patients undergoing MRI examinations at 1.5 T/64 MHz or 3 T/128 MHz. [23].

Six samples of the lead with receiver were attached in three different orientations (i.e., axial, sagittal, and coronal orientations, two in each position) to a plastic copper-sulfate- lled phantom. Porous paper tape (MicroPore, 3M) was used to secure the samples to the phantom. The orientations of the implants were selected to encompass possible clinical placement scenarios for this implant in a patient undergoing an MRI procedure [23]. MRI was performed at 1.5 T/64 MHz (Magnetom) and 3 T/128 MHz (Excite) using a transmit-receive RF body coil and eight different pulse sequences running sequentially, as previously described [23] (Table 1). Functional testing of each lead with receiver was performed before and after the exposures in accordance with the manufacturer's speci cations. The ndings were characterized as either "pass" or "fail" with respect to possible functional disturbances.

Assessment of Artifacts

To evaluate the lead with receiver for artifacts on MRI, a slightly curved sample was attached to a plastic frame and then placed into a gadolinium-infused, saline- lled plastic phantom to assess artifacts at 3 T. MRI was performed using a 3-T system (Excite, HDx, Software 14 ×.M5), as previously described [17, 22, 23]. Similar to the tests for magnetic eld interactions, testing artifacts for an implant or device at 3 T is deemed a worst-case scenario because it represents the highest eld strength commonly used in the clinical setting. [15]. MR images were obtained using T1-weighted, spin-echo, and gradient-echo pulse sequences [17, 22, 23] (Table 2). The imaging planes were oriented to the short and long axes of the lead with receiver. The frequency-encoding direction was parallel to the plane of imaging.

Planimetry software was used to measure the maximum or worst-case artifact areas [17, 22, 23]. The accuracy of this measurement method is plus or minus 10%. The image display parameters were used in a consistent manner to obtain valid measurements for the artifacts [17, 22, 23].

TABLE 1: MRI Sequences and Parameters Used to Assess Functional Disturbance of Lead With Receiver

Parameter	Spin-Echo		Fast Spin-Echo		Gradient-Echo		3D FGE	EPI
	T1-Weighted	T2-Weighted	T1-Weighted	T2-Weighted	3D	MTC		
TR	700	3000	700	5000	20	628	3.7	3400
TE	10	100	9	113	5	10	1.1	103
Flip angle (°)	NA	NA	NA	NA	25	25	NA	NA
FOV	30 cm	30 cm	30 cm	30 cm	30 cm	30 cm	30 cm	30 cm
Matrix size	256 × 256	256 × 256	256 × 256	256 × 256	256 × 256	256 × 256	256 × 256	256 × 256
Slice thickness (mm)	10	10	10	10	3	10	3	10
Section gap (mm)	1	1	1	1	0.6	1	0.6	1
Imaging plane	Axial	Axial	Axial	Axial	VR	Axial	VR	Axial
Imaging time (min)	1	1	1	1	1	1	1	1

Note—Testing was performed either at 1.5 T/64 MHz or 3 T/128 MHz. MTC = magnetization transfer contrast, FGE = fast gradient-echo, EPI = echo-planar imaging, NA = not applicable, VR = volume-rendered.

TABLE 2: Artifact Test Results of the Lead With Receiver at 3 T/128 MHz

Parameter	MRI Sequence			
	T1-Weighted Spin-Echo		Gradient-Echo	
	Parallel (Long Axis)	Perpendicular (Short Axis)	Parallel (Long Axis)	Perpendicular (Short Axis)
Signal void artifact (mm^2)	1672	304	2682	882
TR	500	500	100	100
TE	20	20	15	15
Flip angle (°)	NA	NA	30	30
Bandwidth	32 kHz	32 kHz	32 kHz	32 kHz
FOV	24 cm	24 cm	24 cm	24 cm
Matrix size	256 × 256	256 × 256	256 × 256	256 × 256
Section thickness (mm)	5	5	5	5

Note—NA = not applicable.

Results

Magnetic Field Interactions

The mean de ection angle was 22°, and the qualitatively determined torque was 0, or no torque for the lead with receiver.

MRI-Related Heating

Phase 1—According to the analysis, because the lead with receiver was capsulated (i.e., insulated) except for the portion containing the metallic electrodes, the location that induced the highest temperature rise along the surface of the lead with receiver was found at the electrodes, particularly the most distal electrode. Thus, this spot was considered the position of maximum heating for the lead with receiver and the most likely location of tissue damage if excessive heating were to occur in association with MRI. The SAR distribution obtained from the analysis showed the heating characteristics of the lead with receiver as well as the path or con guration to position the lead with receiver, which was subsequently used for experimental testing in phase 2.

Phase 2—The MRI-related heating evaluation for the lead with receiver found that the greatest amount of heating at 1.5 T/64 MHz and 3 T/128 MHz was 3.8°C and 11.3°C, respectively. The highest background temperature changes at 1.5 T/64 MHz and 3 T/128 MHz were 1.3°C and 1.5°C, respectively.

Evaluation of Possible Functional Disturbances

The evaluation of the functional aspects of the samples of the lead with receiver associated with exposures to the two different MRI conditions revealed that each sample retained its full operational capacity, thus successfully passing the criteria set by the manufacturer. Notably, there was no signi cant change in the power characteristics insofar as the nominal power level characterization remained the same for each lead with receiver.

Artifacts

Artifacts caused by the lead with receiver appeared on MR images as localized signal voids (i.e., signal loss) that corresponded to the size and shape of the device (Table 2). The gradient-echo pulse sequence produced larger artifacts than the T1-weighted, spin-echo pulse sequence. The maximum artifact size associated with the gradient-echo pulse sequence extended 10 mm linearly relative to the size and shape of the lead (Fig. 2).

Discussion

For more than 3 decades, SCS has been a vital therapy for the treatment of chronic pain as well as other medical conditions [1–5, 8–10]. MRI is an essential imaging modality that is frequently needed by patients implanted with neuromodulation systems used for SCS, which often creates problems because of scanning limitations that typically exist for devices designed with conventional components [1, 12, 15]. Wirelessly powered leads for SCS not only represent a practical option for patients but also have fewer issues with respect to their clinical utilization and the use of MRI technology in implanted individuals [1, 9, 10, 17, 24].

An advantage of using a wirelessly powered lead for SCS is the elimination of components that are required by traditional systems, namely the pulse generators and longer leads [9, 10]. Patient movement tends to be restricted because of implanted pulse generators with the longer leads, with certain complications resulting from their presence [7–9]. Because a wirelessly powered lead used for SCS has circuitry small enough to be fully contained within the lead, it can be implanted through a 13-gauge needle via a minimally invasive approach. Thus, bene ts of a wirelessly powered lead system include decreased implantation procedural time, lower risk of infection, reduced overall costs compared with conventional neuromodulation systems and, because of its unique design features, diminished limitations for patients undergoing MRI [1, 6–10, 17].

A previous study performed on an older, less sophisticated lead (i.e., with four electrodes and no receiver) revealed that the device was acceptable for patients using 1.5-T/64-MHz or 3-T/128-MHz MRI conditions [17]. In the

Fig. 2—Gradient-echo MR image shows artifacts at 3 T for lead with receiver. Smaller artifact (i.e., signal loss) is seen at location of electrodes (left side, distal portion) and larger artifact at position of receiver (right side, proximal portion).

present investigation, the newer version of the stimulator incorporates a receiver that has eight electrodes. Importantly, there is no limit to the number of electrodes that can be powered, permitting additional therapeutic options for pain management when using this device.

Magnetic Field Interactions

The lead with receiver showed relatively minor magnetic eld interactions (i.e., 22° de ection angle and no torque) at 3 T. According to ASTM F2052-15, if the de ection angle is less than 45°, magnetically induced translational attraction is less than the force of gravity and thus poses no greater impact than normal daily activity in Earth's gravitational eld [14]. Therefore, this implant will not pose a risk to a patient undergoing MRI at 3 T or less with respect to translational attraction or rotational movement [14, 15].

MRI-Related Heating

The MRI-related heating of an implant, particularly the lead associated with a neuromodulation system, can cause a serious burn injury in a patient [1, 15]. As part of the MRI-related heating assessment performed on the lead with receiver, it was necessary to conduct numerical simulations and analytic modeling to determine the worst-case con guration (or path) that results in the greatest temperature elevation for this device because of the various implantation scenarios that can result in different heating effects [15, 20, 21, 25]. Furthermore, because MRI-related heating is not uniformly distributed over the surface of an implant, the location of the maximum heating can be identi ed computationally [20, 21, 25]. Therefore, the ndings from the analysis conducted in phase 1 of the heating assessment were used to determine the worst-case con guration and the site of the greatest heating for the lead with receiver to guide set-up for experimental testing in phase 2.

Findings from the experimental testing indicated that the lead with receiver had the highest temperature rise of 3.8°C at 1.5 T/64 MHz and 11.3°C at 3 T/128 MHz in association with relatively high whole body–averaged SAR levels. These ndings were not surprising given that the incident wavelength (i.e., the frequency of the transmitted RF) relative to the length of the lead can result in substantially different heating levels [1, 15, 17, 20, 21, 25].

To ensure patient safety and in consideration of the fact that the implant heating that occurs during MRI scales to SAR levels, the following guidelines are recommended: MRI performed at 1.5 T/64 MHz must be conducted at a whole body–averaged SAR of 2.0 W/kg (i.e., the normal operating mode of operation for the MRI system); at 3 T/128 MHz the whole body–averaged SAR must be limited to 0.3 W/kg over the torso and 2 W/kg over other areas of the body (i.e., to include a margin of safety). The temperature rise for an implant subjected to MRI-related heating can be adjusted or scaled to a particular whole body–averaged SAR level [15, 16]. Thus, adjusting the whole body–averaged SAR levels as indicated to prevent excessive heating result in temperature rises of 3.6°C and 1.2°C, respectively. These recommended levels will ensure that the temperature rise of the lead with receiver will not exceed a physiologically consequential value during MRI. Furthermore, during the heating assessment, a static medium (i.e., no perfusion) was used, such that an additional margin of safety may be presumed with regard to possible MRI-related heating issues for this implant.

Functional Disturbances

The assessment of possible functional disturbances for samples of the lead with receiver showed no issues from exposure to 1.5-T and 3-T conditions. One of the factors presumed to be responsible for this desirable nding relates to the design of the lead with receiver. This implant has an application-speci c integrated circuit set to be off, which must be programmed by a con guration initialization pulse to deliver stimulation to one or more electrodes. Any signal that is not a con guration request, such as a signal caused by activation of the MRI system's electromagnetic elds, does not trigger a response in the circuitry because the signal generated by the pulse sequences or exposure conditions would be routed to the integrated circuit without the con guration initialization pulse details.

Artifacts

The artifacts seen at 3 T/128 MHz for the lead with receiver varied with respect to the position on this implant. They were smaller at the location of the electrodes (distal portion) and larger at the positions of the antenna and circuit board (proximal portion), which was related to the materials used for those portions of the lead. Therefore, image quality may be compromised if the area of interest is in the same location or relatively close to the position of this lead with receiver. Thus, optimizing the parameters that reduce artifacts is recommended to avoid potential issues [15].

Possible Limitations

The testing described in this investigation involved two MRI systems: 1.5 T/64 MHz and 3 T/128 MHz. Adverse interactions may be possible in patients undergoing MRI in scanners operating below or above these static magnetic eld strengths and frequencies because the eld distribution and the wavelength inside the patient can be substantially different. For example, an unfortunate case study emphasized the danger of deep brain stimulation leads and electrodes interacting with MRI when safe operating conditions were not observed [26]. This serious incident illustrates that although MRI examinations may be performed in patients with deep brain stimulation devices under specific, well-controlled MRI conditions, any deviation may result in substantial consequences for the patient [26–28].

Furthermore, the safety of performing MRI in a patient with this lead and receiver and another electronically activated implant (e.g., deep brain, spinal cord or vagus nerve stimulation systems) is unknown. Caution is warranted in these situations, and MRI should only be performed after careful consideration of the risks and bene ts.

Conclusion

Comprehensive testing performed to assess MRI issues for the lead with receiver found no substantial concerns related to the conditions that were applied. Therefore, using proper terminology [15, 16], this device is designated as "MR-Conditional" (de ned as an item that has been demonstrated to pose no known hazards in a speci ed MRI environment according to speci c conditions of use). The following safety guidelines based on the ndings of this investigation should be carefully followed to ensure the safety of scanning a patient implanted with this lead with receiver.

First, the external components associated with this device must be removed from the patient before being allowed into the MRI system room.

Second, the static magnetic eld should be either 1.5 T or 3 T only.

Third, at 1.5 T/64 MHz, the maximum whole body–averaged SAR must be 2.0 W/kg for 15 minutes of scanning per pulse sequence.

Fourth, at 3 T/128 MHz, the maximum whole body–averaged SAR must be 0.3 W/kg over the torso and 2 W/kg for other areas of the body for 15 minutes of scanning per pulse sequence, adjusting to a lower SAR value to prevent an excessive temperature rise.

Fifth, there is no restriction on the position of the lead with receiver relative to the type of transmit RF coil that is used for MRI.

Acknowledgments

We thank Laura Perryman and Benjamin Speck at Stimwave Technologies, Inc., for their advice and for providing samples for this project and Sam Valencerina for his assistance with the MRI investigations.

References

1. Manker SG, Shellock FG. MRI safety and neuromodulation systems. In: Krames ES, Peckham PH, Rezai AR, eds. *Neuromodulation*, 2nd ed. London, UK: Academic Press, 2018:315–337
2. Krames ES, Peckham PH, Rezai A, Aboelsaad F. What is neuromodulation? In: Krames ES, Peckham PH, Rezai AR, eds. *Neuromodulation*, 2nd ed. London, UK: Academic Press, 2018;1:19–23
3. Jeon YH. Spinal cord stimulation in pain management: a review. *Korean J Pain* 2012; 25:143–150
4. Weiner RL, Yeung A, Montes Garcia C, Tyler Perryman L, Speck B. Treatment of FBSS low back pain with a novel percutaneous DRG wireless stimulator: pilot and feasibility study. *Pain Med* 2016; 17:1911–1916
5. Doleys DM, Dolce JJ. Psychological issues and evaluation for patients undergoing implantable technology. In: Krames ES, Peckham PH, Rezai AR, eds. *Neuromodulation*, 2nd ed. London, UK: Academic Press, 2018:15–24
6. Krames ES, Mogilner AY, Duarte RV, Thomson SJ, Piedemonte F. Reimbursements for neuromodulation therapies and technologies. In: Krames ES, Peckham PH, Rezai AR, eds. *Neuromodulation*, 2nd ed. London, UK: Academic Press, 2018:1687–1690
7. Speck B. *Complications and risks associated with implantable pulse generators (IPGs): white paper.* London, UK: Stimwave Technologies, Inc., 2016
8. Verrills P, Sinclair C, Barnard A. A review of spinal cord stimulation systems for chronic pain. *J Pain Res* 2016; 9:481–492
9. Perryman LT, Larson P, Glaser J. Tissue depth study for a fully implantable, remotely powered and programmable wireless neural stimulator. *Int J Nano Stud Technol* 2016; 3(S2):1–6
10. Perryman LT, Speck B, Garcia CM, Rashbaum R. Injectable spinal cord stimulator system: pilot study. *Tech Reg Anesth Pain Manage* 2012; 16:102–105
11. Sammartino F, Krishna V, Rezai AR. MRI and fMRI for neuromodulation. In: Krames ES, Peckham PH, Rezai AR, eds. *Neuromodulation*, 2nd ed. London, UK: Academic Press, 2018:121–127
12. Desai MJ, Hargens LM, Breitenfeldt MD, et al. The rate of magnetic resonance imaging in patients with spinal cord stimulation. *Spine* 2015; 40:E531–E537
13. American Society for Testing and Materials (ASTM) International. *Standard practice for marking medical devices and other items for safety in the magnetic resonance environment*. West Conshohocken, PA: ASTM International, 2013: ASTM F2503-13
14. American Society for Testing and Materials (ASTM) International. *Standard test method for measurement of magnetically induced displacement force on passive implants in the magnetic resonance environment*. West Conshohocken, PA: ASTM International, 2015: ASTM F2052-15
15. Shellock FG. *Reference manual for magnetic resonance safety, implants, and devices.* Los Angeles, CA: Biomedical Research Publishing Group, 2019
16. Shellock FG, Woods TO, Crues JV 3rd. MR labeling information for implants and devices: explanation of terminology. *Radiology* 2009; 253:26–30
17. Shellock FG, Audet-Grif n AJ. Evaluation of magnetic resonance imaging issues for a wirelessly powered lead used for epidural, spinal cord stimulation. *Neuromodulation* 2014; 17:334–339; discussion, 339
18. American Society for Testing and Materials (ASTM) International. *Standard test method for measurement of radio frequency induced heating near passive implants during magnetic resonance imaging.* West Conshohocken, PA: ASTM International, 2011: ASTM F2182–11a
19. International Organization for Standardization. *ISO/TS 10974:2012—assessment of the safety of magnetic resonance imaging for patients with an active implantable medical device*. Geneva, Switzerland: International Organization for Standardization, 2012
20. Feng S, Qiang R, Kainz W, Chen J. A technique to evaluate MRI-induced electric elds at the ends of practical implanted wire. *IEEE Trans Microw Theory Tech* 2015; 63:305–313
21. Liu Y, Chen J, Shellock FG, Kainz W. Computational and experimental studies of an orthopedic implant: MRI-related heating at 1.5-T/64-MHz and 3-T/128-MHz. *J Magn Reson Imaging* 2013; 37:491–497
22. Weiland JD, Faraji B, Greenberg RJ, Humayun MS, Shellock FG. Assessment of MRI issues for the Argus II retinal prosthesis. *Magn Reson Imaging* 2012; 30:382–389
23. Shellock FG, Knebel J, Prat AD. Evaluation of MRI issues for a new neurological implant, the Sensor Reservoir. *Magn Reson Imaging* 2013; 31:1245–1250
24. Parker JL, Cameron T. Technology for peripheral nerve stimulation. In: Slavin KV, ed. *Stimulation of the peripheral nervous system: the neuromodulation frontier.* Basel, Switzerland: Karger, 2016:189–191
25. Center for Devices and Radiological Health. *Assessment of radiofrequency-induced heating in the magnetic resonance environment for multiconfiguration passive medical devices. guidance for industry and Food and Drug Administration staff.* Rockville, MD: U.S. Food and Drug Administration, 2016
26. Henderson JM, Tkach J, Phillips M, Baker K, Shellock FG, Rezai AR. Permanent neurological de cit related to magnetic resonance imaging in a patient with implanted deep brain stimulation electrodes for Parkinson's disease: case report. *Neurosurgery* 2005; 57:E1063; discussion, E1063
27. Rezai AR, Baker KB, Tkach JA, et al. Is magnetic resonance imaging safe for patients with neurostimulation systems used for deep brain stimulation? *Neurosurgery* 2005; 57:1056–1062; discussion, 1056–1062
28. Rezai AR, Phillips M, Baker KB, et al. Neurostimulation system used for deep brain stimulation (DBS): MR safety issues and implications of failing to follow safety recommendations. *Invest Radiol* 2004; 39:300–303